 CMC, vol.44, no.3, pp.205-221, 2014

# Wrinkling Analysis in a Film Bonded to a Compressible Compliant Substrate in Large Deformation

**Zhicheng Ou[1], Xiaohu Yao[1], Xiaoqing Zhang[1,2] and Xuejun Fan[3]**

**Abstract:** The buckling of a thin film on a compressible compliant substrate in large deformation is studied. A finite-deformation theory is developed to model the film and the substrate under different original strain-free configurations. The neo-Hookean constitutive relation is applied to describe the substrate. Through the perturbation analysis, the analytical solution for this highly nonlinear system is obtained. The buckling wave number, amplitude and critical condition are obtained. Comparing with the traditional linear model, the buckling amplitude decreases. The wave number increases and relates to the prestrain. With the increment of Poisson's ratio of the substrate, the buckling wave number increases, but the amplitude decreases. The displacements near the interface are different in two models.

**Keywords:** film, substrate, buckling, large deformation, neo-Hookean.

## 1 Introduction

Stretchable electronics is now attracting considerable attention, due to its broad range of applications, such as microelectronics, medicine, clothing and military. Comparing with traditional printing and flat panel displays, flexible displays have both of their advantages, which are soft and portable, and able to store more information [Rogers and Bao (2002)]. The flexible sensors integrated into the clothes can monitor the health information of human body [Wagner, Lacour, Jones, Hsu, Sturm, Li and Suo (2004)]. Travelers and athletes can carry flexible solar panels for power [Schubert and Werner (2006)]. To make the device stretchable, buckling of a stiff film bound to a compliant substrate is applied. Khang, Jiang, Huang and Rogers (2006) produced a stretchable form of silicon based on a PDMS substrate. It is periodic and wavelike in microscale. It can be reversibly stretched and compressed in large deformation without damage.

[1] School of Civil Engineering and Transportation, South China University of Technology, Guangzhou 510640, PR China.
[2] Corresponding author. E-mail: tcqzhang@scut.edu.cn
[3] Department of Mechanical Engineering, Lamar University, Beaumont, TX, 77710, USA.

Huang, Hong and Suo (2005) developed a model of a stiff elastic thin film on a compliant elastic substrate subjected to an axial strain. They obtained the buckling wavelength and amplitude of the film and developed a method to reveal the two-dimensional patterns. Huang (2005) studied the wrinkling process of an elastic film on a viscoelastic layer. Linear perturbation analysis is conducted to reveal the kinetics of wrinkling in the film. Huang and Suo (2002) studied the wrinkling process of this system by using the lubrication theory for the viscous flow and the nonlinear plate theory for the elastic film, and presented a more rigorous analysis for all thickness range of the viscous layer. Im and Huang (2008) considered the wrinkle patterns of anisotropic crystal films on viscoelastic substrates. Jiang, Khang, Fei, Kim, Huang, Xiao and Rogers (2008) considered the finite width effect of thin-films buckling on compliant substrate. Song, Jiang, Choi, Khang, Huang and Rogers (2008) studied the two-dimensional buckling including checkerboard and herringbone modes, and found that the herringbone mode corresponds to the lowest energy, as observed in experiments. Chen and Hutchinson (2004) also showed that the herringbone mode constituted a minimum energy configuration among a limited set of competing modes. Audoly and Boudaoud (2008) studied the secondary instabilities of these modes and presented a weakly nonlinear post-buckling analysis. They found that the square checkerboard mode was optimal just above the threshold under equi-biaxial prestrain. Cai, Breid, Crosby, Suo and Hutchinson (2011) studied the thin stiff films on compliant elastic substrates subjected to equi-biaxial compressive stress states, which were observed to buckle into various periodic patterns including checkerboard, hexagonal and herringbone. For flat films, the checkerboard mode was preferred only above the threshold. Nair, Farkas and Kriz (2008) studied of size effects and deformation of thin films due to nanoindentation using molecular dynamics simulations. Kurapati, Lu and Yang (2010) used the finite element method to analyze the spherical indentation of elastic film and substrate structures.

In previous studies, the substrate is usually described by small deformation theory and linear elastic constitutive relation. But when the structure are subjected to large loads and buckles into large deformation, the small deformation hypothesis is no longer applicable. Song, Jiang, Liu, Khang, Huang, Rogers, Lu and Koh (2008) analyzed the large deformation of this structure by perturbation method. The original strain-free configuration of the film was considered. The finite strain theory and hyperelasticity constitutive relation were applied to describe the substrate. For the incompressible substrate, the buckling features were deduced analytically and coincided well with the experiments and simulations. Zhu, Zhou and Fan (2014) studied rupture and instability of soft films due to moisture vaporization in microelectronic devices. Neo-Hookean, Mooney–Rivlin, and Ogden's models were used

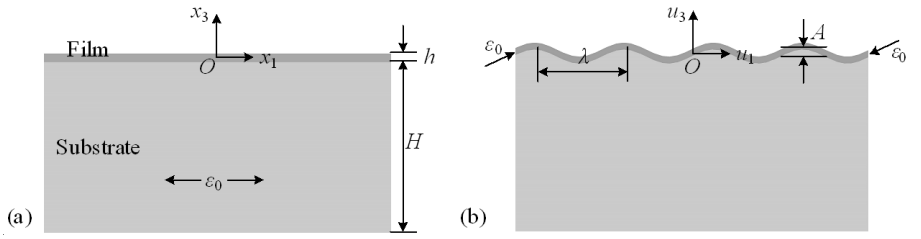


Figure 1: A stiff thin film on a compliant thick substrate: (a) The film is bonded to a pre-strained substrate; (b) The structure buckles after releasing the prestrain.

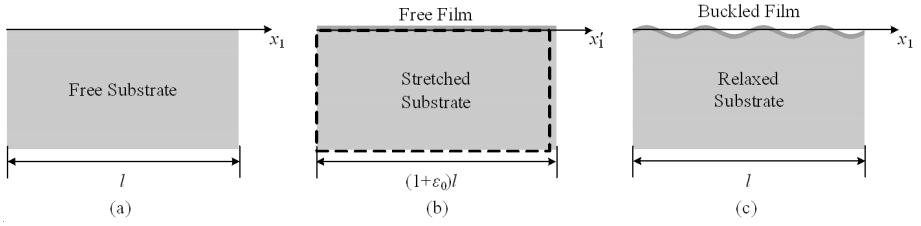


Figure 2: The buckling process and coordinate systems (a) Free substrate; (b) Stretched substrate and free film; (c) Relaxed substrate and buckled film.

In this paper, two models are compared:

(1) Linear model. The small deformation theory and linear elasticity constitutive relation, Hookean law, are applied to describe the substrate. The same coordinate system under the strain-free configuration of the substrate is applied to describe the film and the substrate.

(2) Nonlinear model. The finite deformation theory and nonlinear hyperelasticity constitutive relation, neo-Hookean law, are applied to describe the substrate. Different coordinate systems under the strain-free configurations of the film and the substrate are applied.

### *2.2 Film*

Under the coordinate system based on the strain-free configuration of the film, Fig. 2(b) the in-plane displacement and deflection in the midplane are denoted by $u_1$ and $u_3$ respectively and they are independent of the thickness. When the film buckles, it undergoes large rotation, so the influence of the deflection should be considered

According to the finite deformation theory, the axial strain is

$$e_{11} = \frac{\mathrm{d}u_1}{\mathrm{d}x_1^0} + \frac{1}{-}$$

### 2.3 Substrate

Under the coordinate system based on the strain-free configuration of the substrate, Fig. 2(a), the displacement is denoted by $u_I$ ($I$=1,3). The deformation gradient is $F_{IJ}= d_{IJ} + u_{IJ}$. The Green strain tensor is

$$E_{IJ} = \frac{1}{2}(u_{I;J} + u_{J;I} + u_{K;I}u_{K;J}) \tag{8}$$

Nonlinear constitutive relation is used,

$$T_{IJ} = \frac{\P W_S}{\P E_{IJ}} \tag{9}$$

where $W_S$ is the strain energy density, and $T_{IJ}$ is the 2nd Piola–Kirchhoff stress. In neo-Hookean constitutive law, the strain energy density has the form that

$$W_S = C_1(J^{2=3}I_1 \quad 3) + D_1(J \quad 1)^2 \tag{10}$$

where the material constants are $C_1 = E/4(1+v)$, $D_1 = E/6(1-2v)$. $J$ is the volume change at a point and equals to the determinant of deformation gradient $\boldsymbol{F}$, $J$= det $\boldsymbol{F} = jd_{IJ}+2E_{IJ}j^{1=2}$. The first invariant $I_1$ is the trace of the left Cauchy-Green strain tensor, that is $I_1$= tr

$$T_1 = F_{11}T_{31} + F_{13}T_{33}; \quad T_3 = F_{31}T_{31} + F_{33}T_{33} \tag{15}$$

The bottom of the substrate is free. At the interface, the shear traction is neglected, and the normal displacement is continuous. The boundary conditions are

$x_3$=x$^+$

$$u_{32} = \frac{p^2}{82944(1-\nu)^5} e^{kx_3} \Big\{ 64kx_3 e^{2kx_3} \cos(3kx_1)(640\nu^5+6544\nu^4-13704\nu^3+10642\nu^2-4403\nu+906) + 3e^{2kx_3}\cos(kx_1)(-24k^3x_3^3(256\nu^2-456\nu+209) + 36k^2x_3^2(5120\nu^4-8960\nu^3+7456\nu^2-4820\nu+1607) + kx_3(40960\nu^5-65536\nu^4+77824\nu^3-121760\nu^2+97544\nu-27161) + 2(87040\nu^5-86528\nu^4+1215-19872\nu^3+48880\nu^2-16823\nu)) - 3\cos(kx_1)(-kx_3(25600\nu^4-39680\nu^3+6816\nu^2+12592\nu-4991) + 2(87040\nu^5-86528\nu^4-19872\nu^3+48880\nu^2-16823\nu+1215)) \Big\}$$

$$u_3 = Ae^{kx_3}(1 \quad kx_3)\cos(kx_1) + \frac{1}{4}A^2k^2e^{2kx_3}x_3[2kx_3 \quad 2 + 3\cos(2kx_1)]$$
$$\frac{1}{32}A^3k^2e^{kx_3}\left[64kx_3e^{2kx_3}\cos(3kx_1) + \cos(kx_1)[13kx_3 + 11\right. \tag{25}$$
$$\left. + e^{2kx_3}(40k^3x_3^3 + 116k^2x_3^2 \quad 71kx_3 \quad 11)\right]$$

And the strain energy is

$$U_S = \frac{1}{6}EkIA^2 \quad 1 + \frac{5}{128}A^2k^2 \tag{26}$$

Song, Jiang, Liu, Khang, Huang, Rogers, Lu and Koh (2008) have the same result

In the nonlinear model, the critical prestrain is deduced by setting $A$=0 in Eq. (28),

$$\tilde{e}_0 = \frac{m^{2=3}}{4\quad m^{2=3}} = \frac{\bar{e}_0}{1\quad \bar{e}_0}\qquad \bar{e}_0 \tag{31}$$

It is only dependent on the material property and approximate to the critical prestrain in the linear model. The ratios between the linear and nonlinear model of the buckling amplitude and wave number are assumed that $\tilde{A}=a\bar{A}$, $\tilde{k}=k\bar{k}$. The variable with a tilde indicates the result in the nonlinear model. From Eq. (29), the buckling government equations (28) can expressed about the parameters $a$ and $k$,

$$\begin{array}{l} (\\ \quad 1\quad x^3k^3 + a^2k^2g(4e_0\quad m^{2=3}) = 0 \\ \quad 3m^{2=3}\quad 12x^2ke_0 + a^2k^2(5gm^{2=3} + 3x^3k)(4e_0\quad m^{2=3}) = 0 \end{array} \tag{32}$$

Neglecting the small quantity $m$ (when the prestrain is not too small), the parameters are solved,

$$k\quad (1 + e_0)[4ge_0(1 + e_0) + 1]^{1=3};\quad a\quad (1 + e_0)^{\ 1/2}[4ge_0(1 + e_0) + 1]^{\ 1=3} \tag{33}$$

By substituting Eqs. (29), (30) and (33) into (27), the minimum potential energy in the nonlinear model $\tilde{U} = f\bar{U}$ is obtained. The ratio between two models is

$$f\quad [4ge_0(1 + e_0) + 1]^{2=3} \tag{34}$$

From Eqs. (29), (30), (33) and (34), the buckling wave number, amplitude and critical prestrain and minimum potential energy are

$$\tilde{k}=\frac{(1 + e_0)z}{h},\ \tilde{A}=\frac{h}{z}\sqrt{\frac{4e_0\quad m^{2/3}}{1 + e_0}},\ \tilde{e}_0=\frac{m^{2/3}}{4\quad m^{2/3}},\ \tilde{U}=\frac{z^2hl\bar{E}_f}{32}(8e_0\quad m^{2=3}) \tag{35}$$

where $z = [4mge_0(1+e_0) + m]^{1=3}$. Different from the linear model, the buckling wave number is not only dependent on the material properties but also the prestrain.

## 4 Discussion

### *4.1 Substrate*

The displacement fields of the substrate in linear and nonlinear models are compared by setting $A$= 3 $m$m, $k$= 0.367 $m$m $^{1}$ ($d$ = 0.175) and $v$= 1/2, as shown in Fig. 3 and 4 At the top of the substrate (the interface to the film), the distribution of displacement in two models is different. The spatial period ($x_1$) in the nonlinear model is nearly two times as that in the linear model. From Eq. (22), the tangential

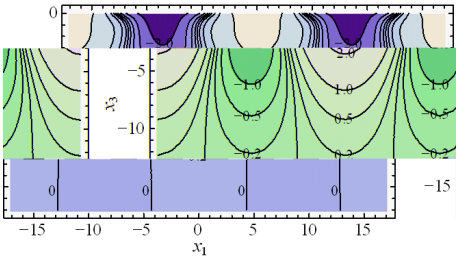


(a) (b)

Figure 3: Displacements (a) $u_1$ and (b) $u_3$ of the substrate in the nonlinear model (*m*m).

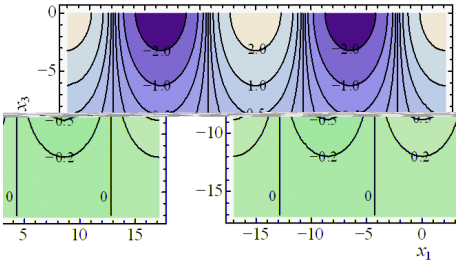


(a) (b)

Figure 4: Displacements (a) $u_1$ and (b) $u_3$ of the substrate in the linear model (*m*m).

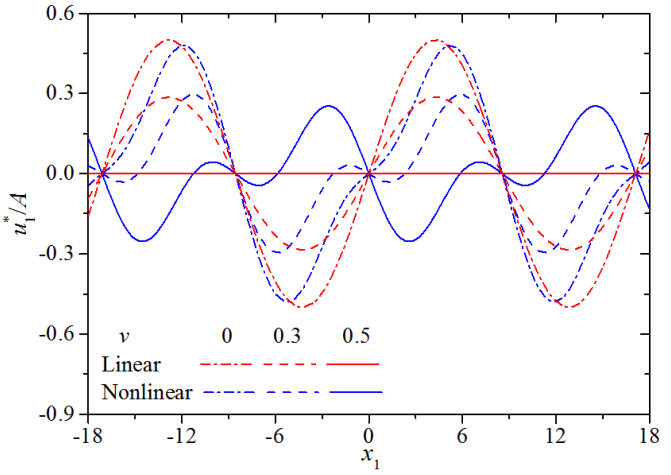


Figure 5: The tangential displacement of the substrate at the interface.

displacement of the substrate at the surface is shown in Fig. 5. When the substrate is incompressible ($v$= 1/2), $u_1$ is zero in the linear model, but nonzero in the nonlinear model.

From Eq. (24), Fig. 6 shows the hyperelastic coefficient $g$ about the Poisson's ratio $v$. It ranges from 0.029 ($v$ 0.31) to 0.047 ($v$= 0.1). From Eq. (23), the ratio of the strain energy of the substrate in two models is $f_s = 1 + gA^2k^2 = 1 + 4gp^2d^2 > 1$. The strain energy of the substrate in the nonlinear model is large than that in the linear model. With the increment of the Poisson's ratio $v$, the energy ratio $f_s$ decreases first and then increases, as shown in Fig. 7(a). When $v$ 0.31, the energy ratio $f_s$ reaches the minimum.With the increment of $d$, the energy ratio $f_s$ increases, as shown in Fig. 7(b).

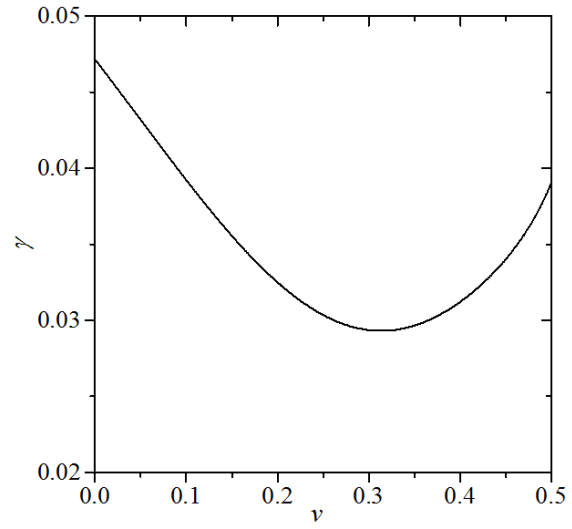


Figure 6: The hyperelastic coefficient $g$.

### 4.2 Buckling

For the silicon film and PDMS substrate, the material and geometric parameters are $E_f$= 130GP45(s0 )]TJ/F87 10.9091 Tf 32.471 0 [(937)]TJ/F100 10.90 Tf 6.905 -1.63039d [(f)]

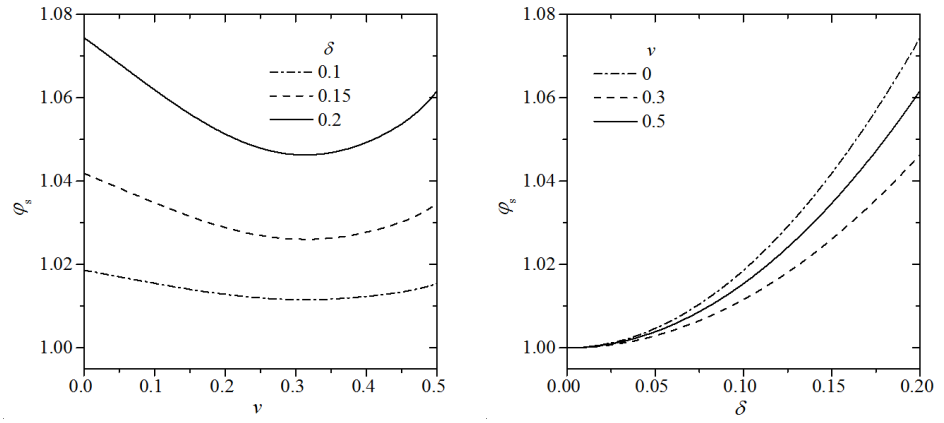


Figure 7: The ratio of substrate's strain energy between two models about (a) the Poisson's ratio and (b) $d = A/l$.

Table 1: The buckling features in two models.

| | $k(\mathrm{mm}^{-1})$ | | | $A(\mathrm{mm})$ | | |
|---|---|---|---|---|---|---|
| $e$ | 0.1 | 0.3 | 0.5 | 0.1 | 0.3 | 0.5 |
| Nonlinear | 0.407 | 0.487 | 0.571 | 1.628 | 2.563 | 3.032 |
| Linear | 0.367 | 0.367 | 0.367 | 1.717 | 2.977 | 3.844 |

shown in Fig. 8(a) The buckling amplitude $A$ in the nonlinear model is less than that in the linear model, as shown in Fig. 8(b) With the increment of Poisson's ratio $v$, the buckling wave number increase, but the amplitude decreases as shown in Fig. 9. The stronger the compressibility of the substrate (the less Poisson's ratio) is, the larger the amplitude and wavelength will be.

Fig. 10 shows the ratios of the buckling wave number $k$, amplitude $a$ and total energy $f$ between two models about the prestrain. With the increment of prestrain, the ratios of buckling wave number $k$ and total energy $f$ are larger than one and increase, but the ratio of amplitude $a$ is less than one and decreases. The ratios of buckling wave number $k$ and amplitude $a$ change significantly when the prestrain increase

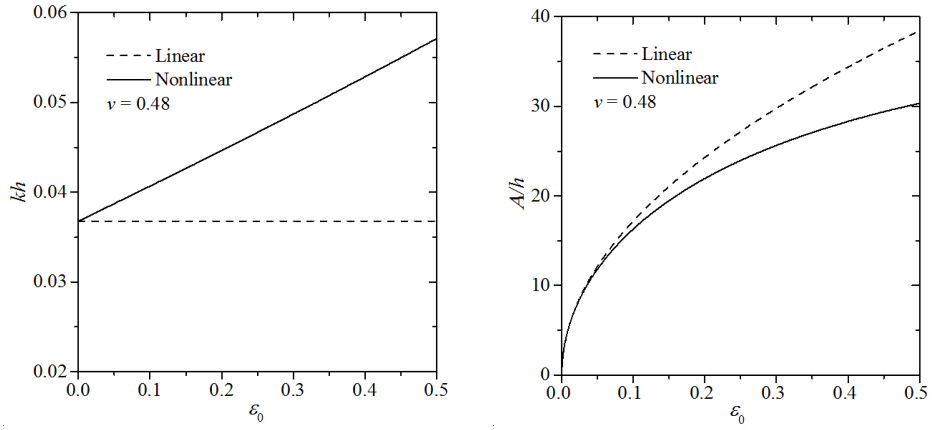


Figure 8: The buckling (a) wave number and (b) amplitude about the prestrain in two models.

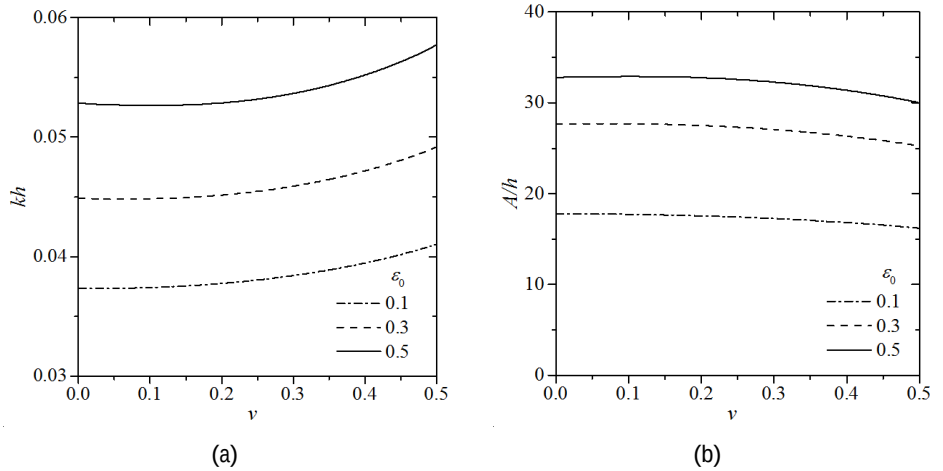


Figure 9: The buckling (a) wave number and (b) amplitude about Poisson's ratio in the nonlinear model.

### *4.3 Film*

From Eq. (5), the midplane displacement of the film consists of two parts. Parts of the wavy displacements caused by buckling in two models are

$$\begin{aligned} \tilde{u}_1^f &= \frac{1}{8} x \tilde{A}^2 \tilde{k} \sin(2\tilde{k} x_1) \quad \text{in nonlinear model} \\ \bar{u}_1^f &= \frac{1}{8} \bar{A}^2 \bar{k} \sin(2\bar{k} x_1) \quad \text{in linear model} \end{aligned} \tag{36}$$

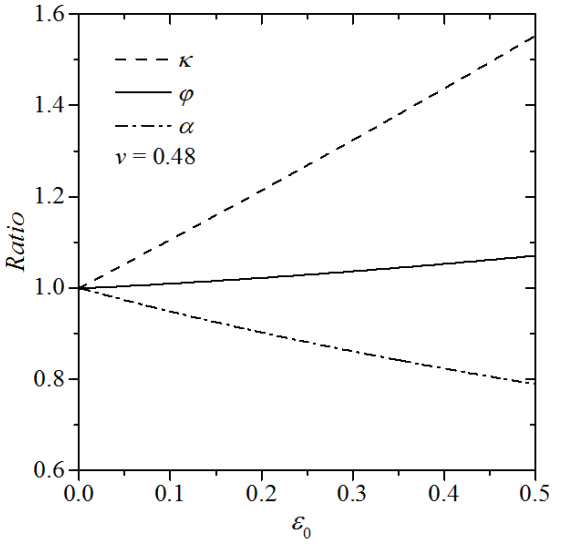


Figure 10: The ratio of wave number $k$, amplitude $a$ and total energy $j$ between two models about the prestrain.

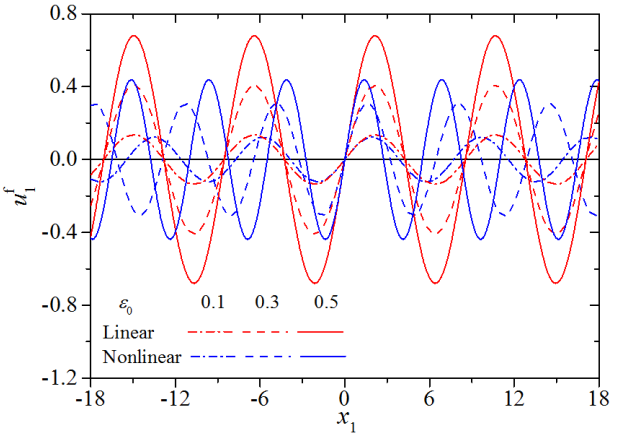


Figure 11: The wavy displacement of the film caused by buckling.

They are shown in Fig. 11 Comparing with the linear model, the prestrain not only influences the amplitude but also the wavelength. The larger the prestrain is, the shorter the wavelength will be in the nonlinear model. The amplitude in the nonlinear model is smaller than that in the linear model, and when the prestrain increase, such difference becomes remarkable.

## 5 Conclusion

This paper studies the buckling of the film and substrate structure in large deformation. A nonlinear model is developed. The film and the substrate are described by finite deformation theory under different original strain-free configurations. The neo-Hookean constitutive relation is applied to describe the substrate Through the perturbation analysis, the displacement of the substrate under a uniaxial prestrain is obtained. The buckling wave number, amplitude and critical condition are obtained by energy method.

The displacement fields near the interface are different in two models. The strain energy of the substrate in the nonlinear model is large than that in the linear model. Comparing with the traditional linear model, the buckling amplitude in the nonlinear model decreases, but the wave number increases and relates to the prestrain. In the nonlinear model, the stronger the compressibility of the substrate is, the larger the buckling amplitude and wavelength will be.

**Acknowledgement:** This work was partially supported by the National Natural Science Foundation of China (Nos. 11372113 and 11472110) New Century Excellent Talents (No. NCET-13-0218).

### References

**Audoly, B.; Boudaoud, A.** (2008): Buckling of a stiff film bound to a compliant substrate–Part I:: Formulation, linear stability of cylindrical patterns, secondary bifurcations. *Journal of the Mechanics and Physics of Solids,* vol. 56, no. 7, pp. 2401-2421.

**Cai, S.; Breid, D.; Crosby, A. J.; Suo, Z.; Hutchinson, J. W.** (2011): Periodic patterns and energy states of buckled films on compliant substrates. *Journal of the Mechanics and Physics of Solids,* vol. 59, no. 5, pp. 1094-1114.

**Chen, X.; Hutchinson, J. W.** (2004): Herringbone buckling patterns of compressed thin films on compliant substrates. *Journal of Applied Mechanics-Transactions of the Asme,* vol. 71, no. 5, pp. 597-603.

**Huang, R.** (2005): Kinetic wrinkling of an elastic film on a viscoelastic substrate. *Journal of the Mechanics and Physics of Solids,* vol. 53, no. 1, pp. 63-89.

**Huang, R.; Suo, Z.** (2002): Instability of a compressed elastic film on a viscous layer. *International Journal of Solids and Structures,* vol. 39, no. 7, pp. 1791-1802.

**Huang, Z. Y.; Hong, W.; Suo, Z.** (2005): Nonlinear analyses of wrinkles in a film

**Im, S. H.; Huang, R.** (2008): Wrinkle patterns of anisotropic crystal films on viscoelastic substrates. *Journal of the Mechanics and Physics of Solids,* vol. 56, no. 12, pp. 3315-3330.